VHEGEN: A vibronic Hamiltonian expansion generator for trigonal and tetragonal polyatomic systems

Robert A. Lang[a,b], Riley J. Hickman[b], Tao Zeng[c,d]

[a]*Department of Physical and Environmental Sciences, University of Toronto Scarborough, Toronto, Ontario, M1C 1A4, Canada*
[b]*Chemical Physics Theory Group, Department of Chemistry, University of Toronto, Toronto, Ontario, M5S 3H6, Canada*
[c]*Department of Chemistry, York University, Toronto, Ontario, M3J 1P3, Canada*
[d]*Department of Chemistry, Carleton University, Ottawa, Ontario, K1S 5B6, Canada*

Abstract

An increasing number of studies in Jahn-Teller and pseudo-Jahn-Teller effects have revealed the importance of vibronic Hamiltonians with high order expansions in vibrational coordinates. This motivates us to present `VHEGEN` (`V`-ibronic `H`-amiltonian `E`-xpansion `GEN`-erator), a Python package that is capable of symbolically generating arbitrarily high order expansion formulas for the vibronic Hamiltonians. The program covers all > 6000 bimodal Jahn-Teller and pseudo-Jahn-Teller problems in trigonal and tetragonal symmetries. The generated expansions are correct, complete, and concise. `VHEGEN` is a useful program for future studies in Jahn-Teller and pseudo-Jahn-Teller effects.

Keywords: Jahn-Teller, pseudo-Jahn-Teller, vibronic coupling, Hamiltonian formalism, Python, symbolic computation

PROGRAM SUMMARY

Program Title: VHEGEN
Licensing provisions: GPLv3
Programming language: Python
Nature of problem: Obtaining correct, complete, and concise high-order expansions of Jahn-Teller and pseudo-Jahn-Teller Hamiltonians in a case-by-case manner is a laborious and error-prone task.

Email address: `tzeng@yorku.ca` (Tao Zeng)

Solution method: We present a Python package to automate the utilization of our recently developed formalisms in obtaining any possible trigonal and tetragonal bimodal (pseudo-)Jahn-Teller vibronic Hamiltonian expanded to arbitrary order in vibrational coordinates.

1. Introduction

Owing to the > 1800 times difference in nuclear and electronic masses, it is often reasonable to assume that the electronic and vibrational motions in a polyatomic system are adiabatically separated, resulting in the classic Born-Oppenheimer approximation [1, 2]. In this approximation, nuclear motion evolves on a single electronic potential energy surface (PES), which is energetically distant from the others. This approximation becomes invalid in the vicinity of electronic degeneracy and pseudo-degeneracy, where the electronic and nuclear motions are strongly coupled, i.e., vibronic coupling [3]. Such non-adiabatic couplings and the consequent transitions between electronic states have been receiving significant attention in recent decades, as they have extensive consequences in spectroscopy, phase transitions, and photophysics [4, 5, 6, 7, 8, 9, 10, 11, 12, 13, 3, 14, 15, 16].

Degeneracy in electronic states can be induced by symmetry of polyatomic systems with the principal axis of rotation (proper or improper) $\geq$ 3-fold. Reversely, for a high-symmetry non-linear polyatomic system, this non-accidental orbital degeneracy distorts its structure and lowers its symmetry. This symmetry lowering due to vibronic coupling between degenerate electronic states and non-totally-symmetric vibrations is the famous Jahn-Teller (JT) effect [17]. Exact degeneracy is not however a mandatory prerequisite for symmetry lowering. Distortion due to the pseudo-Jahn-Teller (pJT) effect [18] occurs for nondegenerate states that are strongly coupled by non-totally-symmetric vibrations. Since their introduction 80 and 60 years ago, respectively, these two effects have been studied extensively [4, 5, 6, 8, 9, 11, 19, 20, 21]. As both molecules and local formations in solids are susceptible to the JT/pJT effects, we use "polyatomic systems" to fully encapsulate the applicability of this work.

Usually, a JT/pJT Hamiltonian is expanded at a high-symmetry configuration in a set of vibrational coordinates and resolved in a set of (pseudo-)degenerate electronic states. To assure Hamiltonian matrix elements are smooth, differentiable functions of the vibrational coordinates, (quasi-)diabatic electronic states are used to resolve the Hamiltonian operator [22, 23, 24, 15, 25, 26]. Traditionally, the expansions in vibrational coordinates are truncated after the second order terms [27]. However, there are several instances in which higher-order expansions are desired, each of which has recently received much attention in the literatures. For example, diabatic potentials are anharmonic and require higher-order expansions when a JT/pJT problem involves bond dissociation [28], and in general when large amplitude vibrations are involved [29, 30, 31, 32, 33, 34, 35, 36, 37]. In experiment, these expansions are needed to understand complicated vibronic spectra [38, 35, 39, 40], and for proper fitting of the spectra to obtain empirical JT/pJT parameters [41, 42]. The need for high-order expansion formulas, along with their vast unavailability, motivates us to endeavor to derive JT/pJT Hamiltonian formalisms up to arbitrary order [43, 44, 45, 46, 47, 48].

The traditional routes to derive high-order JT/pJT Hamiltonians using the Wigner-Eckart Theorem [49, 50] or extracting the totally symmetric component in an all-inclusive expansion are laborious and error-prone, and hence in practice, impose an upper limit on the order of the expansions. Combining the idea of descent in symmetry [51], the root-branch approach, and the modularized approache, we show that it is feasible to derive analytical formulas of arbitrary order expansions of JT/pJT Hamiltonians for one class of axial symmetry and summarize the results in just a few lookup tables. For instance, all 5150 bimodal JT/pJT problems of the seven tetragonal point groups are covered in Ref. 44. If one needs, say, the thirtieth order JT Hamiltonian of the $E_g \otimes (e_u + b_{2u})$ problem in D_{4h} symmetry, we, in a matter of minutes, give the answer: there are two unique matrix elements and they take the following expansions:

$$H_{+_g+_g} = a^{r,4k}_{2I,2K} w^{2I} \rho^{4k+2K} \cos(4k\phi) \text{ with } 2I + 4k + 2K \leq 30; \quad (1)$$

$$H_{+_g-_g} = b^{r,4k+2}_{2I,2K} w^{2I} \rho^{|4k+2|+2K} e^{i(4k+2)\phi} \text{ with } 2I + |4k+2| + 2K \leq 30. \quad (2)$$

Throughout this work, Einstein's convention of summing over duplicate indices is followed, and coefficients denoted by superscripts r and i, e.g., $b^{r,4k+2}_{2I,2K}$ and $b^{i,4k+2}_{2I,2K}$, are real-valued. Summation (power) indices take nonnegative integer values unless they are within the absolute value symbol (e.g., the k in Eq. 2). In these cases, the indices also take negative integer values. In these two equations, ρ and ϕ are polar coordinates of the e_u mode, and w is the coordinate of the b_{2u} vibration.

The two approaches mentioned above are of critical importance in the efficient derivation of the expansion formulas. The root-branch approach allows us to obtain expansion formulas (i.e., branch formulas) for high symmetry (e.g., C_{3v}) by imposing constraints on those (i.e., root formulas) for low symmetry (e.g., C_3). Therefore, we only need to derive actual formulas for the lowest root symmetries, C_3 and C_4 for trigonal and tetragonal, respectively, and the constraints. The modularized approach allows us to select expansion formulas according to symmetry eigenvalues of the matrix elements. Consequently, different matrix elements can adopt the same expansion formulas, while with different expansion coefficients.

Certainly, the present streamline of obtaining the order-by-order, term-by-term expansions of a JT/pJT Hamiltonian by using the lookup tables is straightforward and less error-prone. However, we still need to manually search the lookup tables to fetch the expansion formulas, find the power indices that satisfy the order constraints (e.g., $2I + 4k + 2K \leq 30$ above), and convert matrix elements of complex-valued electronic states (e.g., $|+_g\rangle$ and $|-_g\rangle$ above) to conventional real-valued states (e.g., $|X_g\rangle$ and $|Y_g\rangle$). This entire process can be automated using a computer, given a powerful symbolic algorithm and that the tabulated JT/pJT formalisms are highly programmable. In this work, we develop a Python package, the `V`-ibronic `H`-amiltonian `E`-xpansion `GEN`-erator (`VHEGEN`). At the push of a button, given an input vibronic interaction and order(s) of expansion, `VHEGEN` can symbolically generate the complete and concise vibronic Hamiltonian expansions for any bimodal JT/pJT problem belonging to any trigonal or tetragonal symmetry, i.e., the C_3, C_{3v}, D_3, C_{3h}, D_{3h}, D_{3d}, C_4, S_4, C_{4v}, D_4, D_{2d}, C_{4h}, and D_{4h} point groups.

The two types of symmetries are first considered because, in addition to their ubiquity [52, 53, 54, 55, 56, 57, 58, 59, 60, 61, 62]: (1) the trigonal are the lowest symmetries that allow JT interaction; (2) the tetragonal symmetries contain all three types of irreducible representations (irreps) for axial symmetries, A, B, and E. The present code thus forms a solid foundation for future development that covers all axial symmetries. Unimodal problems are special cases of bimodal analogues with one set of coordinates being set to 0. They are thus also covered by the program. In the current stage, we are content with bimodal problems because: (1) it is usually adequate to consider up to two vibrational modes on the same footing; (2) problems involving more than two modes can be approximated as a composite of bimodal subproblems; (3) given bimodal expansions, it is straightforward to manually obtain expansions of more than two vibrational modes.

2. Settings and symbols

We use upper case symbols to label electronic states and lower case symbols to label vibrational modes. Γ and γ are used to denote generic Mulliken symbols in upper and lower cases, respectively. For doubly degenerate E-type states in trigonal symmetries, the two real-valued component states $|X\rangle$ and $|Y\rangle$ are defined so that they transform under $\hat{C}_3$ as

$$\hat{C}_3 |X\rangle = -\frac{1}{2} |X\rangle + \frac{\sqrt{3}}{2} |Y\rangle ; \hat{C}_3 |Y\rangle = -\frac{\sqrt{3}}{2} |X\rangle - \frac{1}{2} |Y\rangle . \tag{3}$$

The analogues in tetragonal symmetries transform under $\hat{C}_4$ (or $\hat{S}_4$) as

$$\hat{C}_4 |X\rangle = |Y\rangle ; \hat{C}_4 |Y\rangle = - |X\rangle . \tag{4}$$

In D_3, D_{3h}, D_{3d}, D_4, D_{2d}, and D_{4h} (C_{3v} and C_{4v}) point groups, $|X\rangle$ is further defined to be symmetric with respect to one of the $\hat{C}_2'$ ($\hat{\sigma}_v$) operations, while $|Y\rangle$ to be antisymmetric with respect to the same $\hat{C}_2'$ ($\hat{\sigma}_v$) operation. $\hat{C}_2'$ means the two-fold rotation perpendicular to the principal axis. Similar definitions are applied to the e_x and e_y components of e-type vibrational modes. x and y are used as vibrational coordinates of a pair of e_x and e_y components. Polar coordinates that are connected to the cartesian coordinates as $x = \rho \cos \phi$ and $y = \rho \sin \phi$ are also used. z and w are coordinates of a- and b-type vibrations, respectively. Examples of E-type states and e-type vibrations that follow the definitions are shown in Figures S1 and S2 in the Supplementary Information for trigonal and tetragonal symmetries, respectively. The real-valued E component states are transformed to complex-valued states for the convenience in deriving expansion formulas:

$$|+\rangle = \frac{1}{\sqrt{2}} (|X\rangle + i |Y\rangle) ; |-\rangle = \frac{1}{\sqrt{2}} (|X\rangle - i |Y\rangle) . \tag{5}$$

These are eigenstates of the rotational operators $\hat{C}_3$, $\hat{C}_4$, or $\hat{S}_4$, with eigenvalues $e^{\mp i \frac{2\pi}{3}}$ for $\hat{C}_3$ and $\mp i$ for the other two operators. In these eigenvalue formulas, the sign selection $\mp$ corresponds to the $|\pm\rangle$ states.

3. The Jahn-Teller and pseudo-Jahn-Teller Hamiltonian formalisms

The derivations of the arbitrary order trigonal and tetragonal JT/pJT formalisms have been given in Refs. 47 and 44 and are hence not repeated.

Here we only present the table-based structure of the formalisms that is relevant for understanding `VHEGEN`. While only the structure of the trigonal formalisms are given, the tetragonal formalisms follow a similar structure. We use the $(E'' + E') \otimes (e'' + a_2')$ pJT problem in D_{3h} symmetry as an example and walk through the streamline of obtaining the expansion formulas of its vibronic Hamiltonian.

The first table, Table 1, summarizes unique matrix elements of each trigonal JT/pJT problem and their eigenvalues of representative symmetry operators: $\hat{C}_3$ for all trigonal point groups, $\hat{C}_2'$ for the D_3, D_{3h}, and D_{3d} point groups, $\hat{\sigma}_v$ for the C_{3v} point group, $\hat{\sigma}_h$ for the C_{3h} and D_{3h} point groups, and $\hat{I}$ for the D_{3d} point group. Please note the isomorphism between D_3 and C_{3v} and the isomorphism between D_{3h} and D_{3d}. In the $(E + E)$ block of the table, we see that there are two unique matrix elements $H_{+''+'}$ and $H_{+''-'}$ for the $(E'' + E') \otimes (e'' + a_2')$ problem. By substituting $''$ into p and $'$ into q, we obtain the four symmetry eigenvalues of these matrix elements: $\chi^{C_3} = 1$, $\left(\chi_{Re}^{C_2'}, \chi_{Im}^{C_2'}\right) = (1, -1)$, and $\chi^{\sigma_h} = -1$ for $H_{+''+'}$; $\chi^{C_3} = e^{-i2\pi/3}$, $\left(\chi_{Re}^{C_2'}, \chi_{Im}^{C_2'}\right) = (1, -1)$, and $\chi^{\sigma_h} = -1$ for $H_{+''-'}$. Please note that the real and imaginary parts of the matrix elements have different $\hat{C}_2'$-eigenvalues, which are denoted by the Re and Im subscripts. This is the result of the non-commutation relation $\left[\hat{C}_3, \hat{C}_2'\right] \neq 0$. Similarly, $\left[\hat{C}_3, \hat{\sigma}_v\right] \neq 0$, and the real and imaginary parts of the matrix elements that are eigenfunctions of $\hat{C}_3$ have different $\hat{\sigma}_v$-eigenvalues. $\chi_{Im}^{C_2'/\sigma_v} = 0$ in the table means that the matrix element is real-valued.

In the second step, we obtain the root expansion formulas according to χ^{C_3} and the vibrational modes in Tables 2 and 3. In the $(e + a)$-block in Table 2, we take the root expansion of $H_{+''+'}$:

$$\begin{aligned} H_{+_\alpha +_\beta} &= \rho^{|3m|+2K} \left[a_{I_1,2K}^{r,3m} z^{I_1} \cos(3m\phi) - a_{I_2,2K}^{i,3m} z^{I_2} \sin(3m\phi) \right. \\ &\quad \left. + i \left(a_{I_1,2K}^{r,3m} z^{I_1} \sin(3m\phi) + a_{I_2,2K}^{i,3m} z^{I_2} \cos(3m\phi) \right) \right]. \end{aligned} \tag{6}$$

Here, the subscripts α and β are to emphasize that the $|+\rangle$ component states arise from different E-type term symbols, E'' and E' in this example. The $(e + a)$-block in Table 3 gives the root expansion of $H_{+''-'}$. Please note that χ^{C_3} of $H_{+''-'}$ is $e^{-i2\pi/3}$, while Table 3 gives the root expansions with $\chi^{C_3} = e^{i2\pi/3}$. Therefore, we need to take the complex conjugate of the root expansion given in the table:

$$\begin{aligned} H_{+\alpha-\beta} &= \rho^{|3n-1|+2K}\left[b^{r,3n-1}_{I_1,2K}z^{I_1}\cos((3n-1)\phi)-b^{i,3n-1}_{I_2,2K}z^{I_2}\sin((3n-1)\phi)\right. \\ &\quad \left.-i\left(b^{r,3n-1}_{I_1,2K}z^{I_1}\sin((3n-1)\phi)+b^{i,3n-1}_{I_2,2K}z^{I_2}\cos((3n-1)\phi)\right)\right]. \end{aligned} \tag{7}$$

Please note that the sign in front of the imaginary unit i has been changed from $+$ in Table 3 to $-$ here. The complex conjugation is all that is needed to obtain expansions of $\chi^{C_3} = e^{-i2\pi/3}$ from the tabulated expansions for $\chi^{C_3} = e^{i2\pi/3}$. It is for this reason that the root expansions of $\chi^{C_3} = e^{-i2\pi/3}$ are not given explicitly. These formulas are called root formulas because constraints are to be imposed on them to get the branch formulas, which are the final expansion formulas for a JT/pJT problems in a symmetry higher than the lowest C_3.

In the third step, we impose the constraints summarized in Tables 4 and 5 on the $H_{+''+'}$ and $H_{+''-'}$ root expansions, respectively. The $(e + a_2)$ entry with $\chi^{C_3} = 1$ and $\left(\chi^{C_2'}_{Re}, \chi^{C_2'}_{Im}\right) = (1, -1)$ in Table 4 is that I_1 has to be even and I_2 has to be odd. The $(e'' + a')$ entry with $\chi^{C_3} = 1$ and $\chi^{\sigma_h/I} = -1$ in Table 5 is $3m$ has to be odd. Imposing all these constraints on Eq. 6, we obtain

$$\begin{aligned} H_{+''+'} &= \rho^{|6m+3|+2K}\left[a^{r,6m+3}_{2I_1,2K}z^{2I_1}\cos\left((6m+3)\,\phi\right)-a^{i,6m+3}_{2I_2+1,2K}z^{2I_2+1}\sin\left((6m+3)\,\phi\right)\right. \\ &\quad \left.+i\left(a^{r,6m+3}_{2I_1,2K}z^{2I_1}\sin\left((6m+3)\,\phi\right)+a^{i,6m+3}_{2I_2+1,2K}z^{2I_2+1}\cos\left((6m+3)\,\phi\right)\right)\right]. \end{aligned} \tag{8}$$

The $(e + a_2)$ entry with $\chi^{C_3} = e^{i2\pi/3}$ and $\left(\chi^{C_2'}_{Re}, \chi^{C_2'}_{Im}\right) = (1, -1)$ in Table 4 is I_1 has to be even and I_2 has to be odd. The $(e'' + a')$ entry with $\chi^{C_3} = e^{i2\pi/3}$ and $\chi^{\sigma_h/I} = -1$ in Table 5 is $3n$ has to be even. Imposing these constraints on Eq. 7, we obtain

$$\begin{aligned} H_{+''-'} &= \rho^{|6n-1|+2K}\left[b^{r,6n-1}_{2I_1,2K}z^{2I_1}\cos\left((6n-1)\,\phi\right)-b^{i,6n-1}_{2I_2+1,2K}z^{2I_2+1}\sin\left((6n-1)\,\phi\right)\right. \\ &\quad \left.-i\left(b^{r,6n-1}_{2I_1,2K}z^{2I_1}\sin\left((6n-1)\,\phi\right)+b^{i,6n-1}_{2I_2+1,2K}z^{2I_2+1}\cos\left((3n-1)\,\phi\right)\right)\right]. \end{aligned} \tag{9}$$

This is the streamline of using the symmetry eigenvalues table, the root formulas tables, and the constraints tables to obtain general expansion formulas of trigonal JT/pJT vibronic Hamiltonian matrix elements. Since real-valued electronic states are usually obtained in non-spin-orbit quantum chemistry calculations, it is desired to convert the expansions of the matrix elements of the complex-valued states to those of the real-valued states using the transformation relations in Eq. 5. This is the fourth step. For the

$(E'' + E') \otimes (e'' + a_2')$ problem, expansions in Eqs. 8 and 9 are transformed to

$$\begin{aligned}
\frac{H_{X''X'} + H_{Y''Y'}}{2} &= Re\left(H_{+''+'}\right) = \rho^{|6m+3|+2K}\left[a^{r,6m+3}_{2I_1,2K} z^{2I_1}\cos\left((6m+3)\,\phi\right)\right. \\
&\quad \left. -a^{i,6m+3}_{2I_2+1,2K} z^{2I_2+1}\sin\left((6m+3)\,\phi\right)\right], \\
\frac{H_{X''X'} - H_{Y''Y'}}{2} &= Re\left(H_{+''-'}\right) = \rho^{|6n-1|+2K}\left[b^{r,6n-1}_{2I_1,2K} z^{2I_1}\cos\left((6n-1)\,\phi\right)\right. \\
&\quad \left. -b^{i,6n-1}_{2I_2+1,2K} z^{2I_2+1}\sin\left((6n-1)\,\phi\right)\right], \\
\frac{H_{X''Y'} + H_{Y''X'}}{2} &= -Im\left(H_{+''-'}\right) = \rho^{|6n-1|+2K}\left[b^{r,6n-1}_{2I_1,2K} z^{2I_1}\sin\left((6n-1)\,\phi\right)\right. \\
&\quad \left. +b^{i,6n-1}_{2I_2+1,2K} z^{2I_2+1}\cos\left((6n-1)\,\phi\right)\right], \\
\frac{H_{X''Y'} - H_{Y''X'}}{2} &= Im\left(H_{+''+'}\right) = \rho^{|6m+3|+2K}\left[a^{r,6m+3}_{2I_1,2K} z^{2I_1}\sin\left((6m+3)\,\phi\right)\right. \\
&\quad \left. +a^{i,6m+3}_{2I_2+1,2K} z^{2I_2+1}\cos\left((6m+3)\,\phi\right)\right]. \qquad (10)
\end{aligned}$$

These expansion formulas can be used for fitting already. If desired, one can express all the sine and cosine factors by products of $\sin\phi$ and $\cos\phi$ and then convert the expansions to cartesian coordinates x and y of the e'' vibration. This is the fifth step. The function of VHEGEN is to do all these five steps and return the final order-by-order, term-by-term expansions of the relevant Hamiltonian matrix elements by a readable output file. The program covers all 908 trigonal and all 5150 tetragonal bimodal pJT and JT problems.

4. Technical overview of VHEGEN

The simple procedure to obtain the expansion formulas presented above enables the generation of a vibronic Hamiltonian of interest in a highly systematic manner, which is implemented in the VHEGEN package. Within this section the core technical details of VHEGEN are presented. The general pipeline from a set of input parameters to the output vibronic Hamiltonian is described in Figure 1. The major procedural steps are described in further detail in the proceeding subsections. In the final subsection, a heuristic example of the procedure from input to output is given for the 3rd order $E' \otimes (e' + a_1'')$ problem in D_{3h} symmetry.

4.1. Obtaining symmetry eigenvalues

The program's input consists of a trigonal or tetragonal point group G, a unimodal or bimodal JT/pJT vibronic problem: $(\Gamma_\alpha + \Gamma_\beta) \otimes (\gamma_\alpha + \gamma_\beta)$,

Table 1: The eigenvalues of representative symmetry operators of the unique elements H_{ij} in trigonal JT/pJT vibronic Hamiltonian matrices. The $\hat{\sigma}_v$- and $\hat{C}_2'$-eigenvalues are given for the real and imaginary parts of the matrix elements separately. k and l stand for the 1 and 2 subscripts when σ_v or C_2' are relevant. p and q stand for the g and u subscipts when I is relevant. Although p and q are placed as subscripts, they also stand for possible $'$ and $''$ superscripts when σ_h is relevant.

Electronic states	ij	χ^{C_3}	$(\chi_{Re}^{\sigma_v/C_2'}, \chi_{Im}^{\sigma_v/C_2'})$	$\chi^{\sigma_h/I}$
$(A+A)/A$	$A_{kp}A_{lq}$	1	$((-1)^{\delta_{kl}+1}, 0)$	$(-1)^{\delta_{pq}+1}$
	$A_{kp}A_{kp}$	1	$(1,0)$	1
$(E+A)$	$+_pA_{kq}$	$e^{i2\pi/3}$	$((-1)^{\delta_{k2}}, (-1)^{\delta_{k1}})$	$(-1)^{\delta_{pq}+1}$
$(E+E)$	$+_p+_q$	1	$(1,-1)$	$(-1)^{\delta_{pq}+1}$
	$+_p-_q$	$e^{-i2\pi/3}$	$(1,-1)$	$(-1)^{\delta_{pq}+1}$
E	$++$	1	$(1,0)$	1
	$+-$	$e^{-i2\pi/3}$	$(1,-1)$	1

Table 2: Root expansion formulas for $\hat{C}_3$-eigenfunctions of the bimodal vibrational coordinates with $\hat{C}_3$-eigenvalue 1. Subscripts α and β are used to differentiate coordinates of the same types of vibrations.

Modes	Expansion Formulas
$(a+a)$	$a^r_{I_1,I_2} z_\alpha^{I_1} z_\beta^{I_2} + i a^i_{I_3,I_4} z_\alpha^{I_3} z_\beta^{I_4}$
$(e+a)$	$a^{3m}_{I,2K} z^I \rho^{\lvert 3m\rvert+2K} e^{i3m\phi} = \rho^{\lvert 3m\rvert+2K}[a^{r,3m}_{I_1,2K} z^{I_1}\cos(3m\phi) - a^{i,3m}_{I_2,2K} z^{I_2}\sin(3m\phi)$ $+i(a^{r,3m}_{I_1,2K} z^{I_1}\sin(3m\phi) + a^{i,3m}_{I_2,2K} z^{I_2}\cos(3m\phi)]$
$(e+e)$	$a^{m,3n}_{2K_1,2K_2}\rho_\alpha^{\lvert m\rvert+2K_1}\rho_\beta^{\lvert 3n-m\rvert+2K_2} e^{i(m\phi_\alpha+(3n-m)\phi_\beta)} = \rho_\alpha^{\lvert m\rvert+2K_1}\rho_\beta^{\lvert 3n-m\rvert+2K_2}$ $[(a^{r,m,3n}_{2K_1,2K_2}\cos(m\phi_\alpha+(3n-m)\phi_\beta) - a^{i,m,3n}_{2K_1,2K_2}\sin(m\phi_\alpha+(3n-m)\phi_\beta)$ $+i(a^{r,m,3n}_{2K_1,2K_2}\sin(m\phi_\alpha+(3n-m)\phi_\beta) + a^{i,m,3n}_{2K_1,2K_2}\cos(m\phi_\alpha+(3n-m)\phi_\beta))]$

$(\Gamma_\alpha + \Gamma_\beta)\otimes\gamma$, $\Gamma\otimes(\gamma_\alpha+\gamma_\beta)$, or $\Gamma\otimes\gamma$, and a range of expansion orders $\{o_i\}$. The set of relevant unique matrix elements and their symmetry eigenvalues $\left(\chi^{C_n,S_n}, \left(\chi_{Re}^{\sigma_v,C_2'}, \chi_{Im}^{\sigma_v,C_2'}\right), \chi^{\sigma_h,I}\right)$ are tabulated in the program and are searched for using the specified electronic term symbol(s), the Γ(s). This step is analogous to obtaining the unique matrix elements and their eigenvalues from Table 1 (for $n = 3$). The input point group determines the number of

Table 3: Root expansion formulas for $\hat{C}_3$-eigenfunctions of the bimodal vibrational coordinates with $\hat{C}_3$-eigenvalue $e^{i2\pi/3}$. The expansion formulas with $\hat{C}_3$-eigenvalue $e^{-i2\pi/3}$ are the complex conjugates of the ones given here. Subscripts α and β are used to differentiate coordinates of the same types of vibrations.

Modes	Expansion Formulas
$(a+a)$	na (not applicable)
$(e+a)$	$b^{3n-1}_{I,2K} z^I \rho^{\lvert 3n-1\rvert+2K} e^{i(3n-1)\phi} = \rho^{\lvert 3n-1\rvert+2K} [b^{r,3n-1}_{I_1,2K} z^{I_1} \cos((3n-1)\phi)$ $-b^{i,3n-1}_{I_2,2K} z^{I_2} \sin((3n-1)\phi) + i(b^{r,3n-1}_{I_1,2K} z^{I_1} \sin((3n-1)\phi) + b^{i,3n-1}_{I_2,2K} z^{I_2} \cos((3n-1)\phi)]$
$(e+e)$	$b^{m,3n-1}_{2K_1,2K_2} \rho_\alpha^{\lvert m\rvert+2K_1} \rho_\beta^{\lvert 3n-1-m\rvert+2K_2} e^{i(m\phi_\alpha+(3n-1-m)\phi_\beta)} = \rho_\alpha^{\lvert m\rvert+2K_1} \rho_\beta^{\lvert 3n-1-m\rvert+2K_2}$ $[(b^{r,m,3n-1}_{2K_1,2K_2} \cos(m\phi_\alpha + (3n-1-m)\phi_\beta) - b^{i,m,3n-1}_{2K_1,2K_2} \sin(m\phi_\alpha + (3n-1-m)\phi_\beta)$ $+i(b^{r,m,3n-1}_{2K_1,2K_2} \sin(m\phi_\alpha + (3n-1-m)\phi_\beta) + b^{i,m,3n-1}_{2K_1,2K_2} \cos(m\phi_\alpha + (3n-1-m)\phi_\beta))]$

symmetry eigenvalues that are needed: χ^{C_n,S_n} for the C_3, C_4, and S_4 groups; plus $\left(\chi^{\sigma_v,C_2'}_{Re}, \chi^{\sigma_v,C_2'}_{Im}\right)$ for the C_{3v}, D_3, C_{4v}, D_{2d}, and D_4 groups; plus $\chi^{\sigma_h,I}$ for the D_{3h}, D_{3d}, and D_{4h} groups. For the C_{3h} and C_{4h} groups, only χ^{C_n} and $\chi^{\sigma_h,I}$ are needed. Naturally, only the eigenvalues of the minimum, representative symmetry operations that determine a point group are needed. Henceforth, we do not differentiate $\hat{C}_4$ and $\hat{S}_4$, keeping in mind that the C_4 and S_4 point groups are isomorphic.

4.2. Obtaining root formulas and constraints

Once the representative symmetry eigenvalues for all unique matrix elements of the problem are known, the root expansion formulas will be obtained. For each unique matrix element, the root formula associated with χ^{C_n} and the vibrational modes is fetched from a predefined formula set. The formula set has expansion formulas with $\chi^{C_3} \in \{1, e^{i\frac{2\pi}{3}}\}$ and $\chi^{C_4} \in \{1, -1, i\}$. For trigonal or tetragonal matrix elements with principal rotation eigenvalue $\chi^{C_3} = e^{-i\frac{2\pi}{3}}$ or $\chi^{C_4} = -i$, the corresponding root formulas are simply complex conjugates of those with $\chi^{C_3} = e^{i\frac{2\pi}{3}}$ or $\chi^{C_4} = i$, respectively.

Additionally, the formula set only contains explicit expansion formulas for bimodal problems. If a unimodal problem is specified, then the second mode γ_β is temporarily set to the totally symmetric a-type mode for duration of the search, which will correspondingly select the $(\gamma_\alpha + a)$ root expansion formula. In the very end, the artificial a vibrational coordinates will be nullified to obtain the unimodal expansion formula of interest.

Table 4: $\hat{\sigma}_v/\hat{C}_2'$-induced constraints on the root expansions in Tables 2 and 3 to give the appropriate $\chi_{Re}^{\sigma_v/C_2'}$ and $\chi_{Im}^{\sigma_v/C_2'}$. When $\chi_{Im}^{\sigma_v/C_2'} = 0$ only the real part of the corresponding root expansion formula should be considered. The meanings of the shorthand notations like nr, na, nz, etc. are given underneath the table.

χ^{C_3}	1			$e^{i2\pi/3}$	
$(\chi_{Re}^{\sigma_v/C_2'}, \chi_{Im}^{\sigma_v/C_2'})$	(1,0)	(-1,0)	(1,-1)	$(1,-1)$	$(-1,1)$
(a_1+a_1)	nr†	na	na	na	na
$(a_1+a_2)^\ddagger$	I_2 e ¶	I_2 o	I_2 e, I_4 o	na	na
(a_2+a_2)	I_1, I_2 § ee/oo	I_1, I_2 £ eo/oe	I_1,I_2 ee/oo, I_3,I_4 eo/oe	na	na
$(e+a_1)$	cos nz #	sin nz	a^r nz	b^r nz	b^i nz
$(e+a_2)$	I_1 e, I_2 o	I_1 o, I_2 e	I_1 e, I_2 o	I_1 e, I_2 o	I_1 o, I_2 e
$(e+e)$	cos nz	sin nz	a^r nz	b^r nz	b^i nz

† "nr" means "no restriction". ‡ For modes whose irreps only differ in subscripts, α-subscripted coordinates in Tables 2 and 3 are for the first mode (a_1 here) and β- for the second mode (a_2 here). ¶ I_2 needs to be even. § I_1 and I_2 need to be both even or both odd. £ When I_1 is even, I_2 must be odd, and vice versa. # "nz" here means only the terms that involve cos factors are nonzero.

For vibronic problems in higher symmetries than C_n, constraints are selected and imposed on the root C_n expansion formulas, according to the matrix elements' $\left(\left(\chi_{Re}^{\sigma_v,C_2'}, \chi_{Im}^{\sigma_v,C_2'}\right), \chi^{\sigma_h,I}\right)$, to obtain the expansions adapted to the higher symmetry. The constraints are tabulated in the program like in Tables 4 and 5. Symmetry constraints are stored in files categorized by: (1) representative symmetry elements; (2) principal rotation eigenvalue χ^{C_n}. Therefore, efficient search for the constraints relevant to the unique matrix elements is achieved. Groups with more than one additional representative symmetry element are treated as composite cases. The tetragonal group D_{4h} is one such example with C_2' and I as the additional symmetry elements, and it is viewed as a composite of the C_{4h} and D_4 point groups, which have the I and C_2' elements, respectively. Therefore, for JT/pJT Hamiltonian expansions in D_{4h} symmetry, we need to impose both the C_{4h} and D_4 constraints

Table 5: $\hat{\sigma}_h/I$-induced constraints on expansions in Tables 2 and 3 to give the appropriate χ^{σ_h}.

χ^{C_3}	1		$e^{i2\pi/3}$	
$\chi^{\sigma_h/I}$	1	-1	1	-1
$(a' + a')$	nr	na	na	na
$(a' + a'')^\dagger$	I_2, I_4 e	I_2, I_4 o	na	na
$(a'' + a'')$	I_1, I_2 ee/oo I_3, I_4 ee/oo	I_1, I_2 eo/oe I_3, I_4 eo/oe	na	na
$(e' + a')$	nr	na	nr	na
$(e' + a'')$	I e	I o	I e	I o
$(e'' + a')$	$3m$ e	$3m$ o	$3n$ o	$3n$ e
$(e'' + a'')$	$3m, I$ ee/oo	$3m, I$ eo/oe	$3n, I$ eo/oe	$3n, I$ ee/oo
$(e' + e')$	nr	na	nr	na
$(e'' + e')$	m e	m o	m e	m o
$(e'' + e'')$	$3n$ e	$3n$ o	$3n$ o	$3n$ e

† For modes whose irreps only differ in subscripts, α-subscripted coordinates in Tables 2 and 3 are for the first mode (a_1 here) and β- for the second mode (a_2 here).

onto the root formulas. In the program, constraints are not applied to the general root formulas explicitly. Rather, they are jointly passed on to the expansion process to select the terms that do not violate them.

4.3. Expansion process

Equipped with the desired orders of expansion, root expansion formulas for the relevant unique matrix elements, and their appropriate constraints (if applicable), `VHEGEN` begins the expansion process. The matrix element expansion process is presented in Algorithm 1 and summarized as follows. Each term appearing in a general expansion formula, e.g., the $a^{r,6m+3}_{2I_1,2K} z^{2I_1} \rho^{|6m+3|+2K} \cos{(6m+3)}\,\phi$ term in Eq. 8, is iterated over through the summation indices (I_1, m, and K for this example) to generate term-by-term expansions at a given order ($2I_1 + |6m+3| + 2K = o_i$, the order of interest). The expansion process begins with generating full sets of summation index values. If the summation indices appear within absolute value

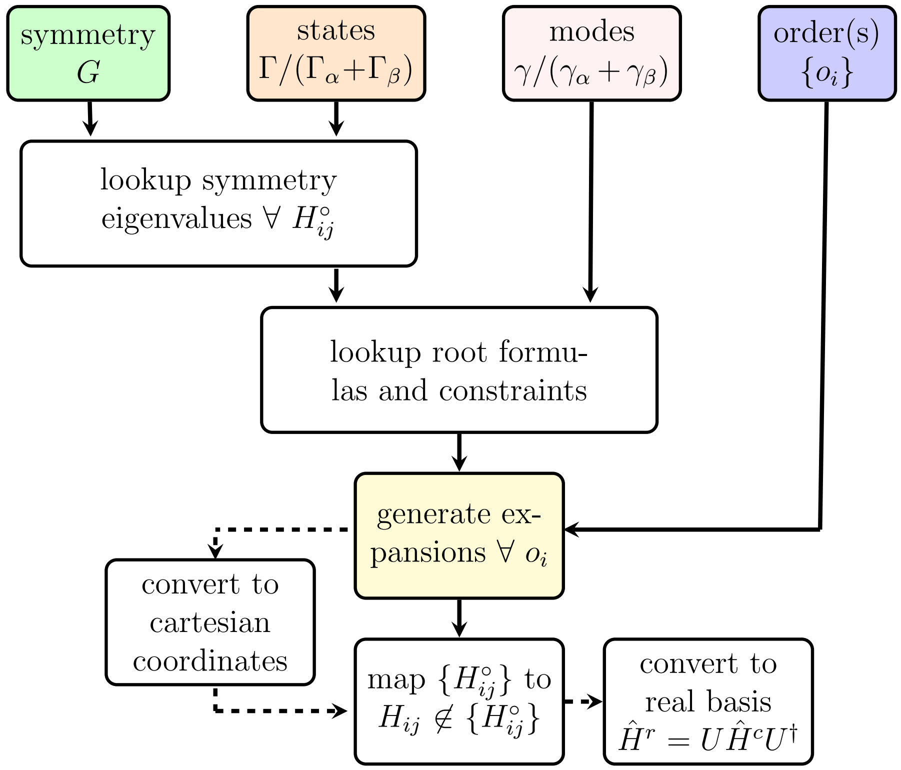

Figure 1: Schematic of the VHEGEN pipeline from input of specific JT/pJT problem to output of vibronic Hamiltonian(s) expanded in vibrational coordinates at the desired order(s). Unique matrix elements are denoted as H°_{ij}. Dashed arrows are used to denote optional processes dependent on the program configuration.

sign in the expansion formulas, they may take any integer within $\{-o_i, -o_i+1, ...o_i-1, o_i\}$. Otherwise, they take values within $\{0, 1, ...o_i-1, o_i\}$. All possible combinations of summation index values are then generated from the full sets of values for each summation index. This set of combinations is denoted S in Algorithm 1. If a combination of summation index values $S_i \in S$ results in the sum of the powers ($2I_1 + |6m+3| + 2K$ of the example here) equal to order o_i, then the combination is checked to see whether it satisfies the constraints relevant to the matrix element of interest. If all relevant constraints are satisfied, then the term with the summation indices in S_i is allowed and thus added to the matrix element expansion. This process is iterated to exhaust all $S_i \in S$.

Care is taken during the expansion process to avoid redundant terms

Algorithm 1

Matrix element expansion process

Input: root formula, constraints, o_i
Output: $H_{ij}^{(o_i)}$

```
for term in root formula:
    generate set of summation index value combinations S
    for S_i in S:
        if term powers = o_i and all constraints satisfied:
            add term to H_ij^(o_i)
        else: discard S_i
```

for cases with $\chi_{Im}^{\sigma_v,C_2'} = 0$. Potential redundancies arise when taking the real part for expansion formulas with summation indices normally allowed to take any integer values. To avoid such redundancies, additional constraints are enforced. For example of the trigonal $(e+e)$ problem with $\chi^{C_3} = 1$ in Table 2

$$a_{2K_1,2K_2}^{m,3n}\rho_\alpha^{|m|+2K_1}\rho_\beta^{|3n-m|+2K_2}e^{i(m\phi_\alpha+(3n-m)\phi_\beta)} = \rho_\alpha^{|m|+2K_1}\rho_\beta^{|3n-m|+2K_2}$$
$$\big[(a_{2K_1,2K_2}^{r,m,3n}\cos(m\phi_\alpha+(3n-m)\phi_\beta) - a_{2K_1,2K_2}^{i,m,3n}\sin(m\phi_\alpha+(3n-m)\phi_\beta)$$
$$+i(a_{2K_1,2K_2}^{r,m,3n}\sin(m\phi_\alpha+(3n-m)\phi_\beta) + a_{2K_1,2K_2}^{i,m,3n}\cos(m\phi_\alpha+(3n-m)\phi_\beta))\big] \quad (11)$$

m and n can take all integer values from negative to positive, since they both appear in the absolute value symbols. However, when only the real part is taken, the formula becomes

$$\rho_\alpha^{|m|+2K_1}\rho_\beta^{|3n-m|+2K_2}\big[(a_{2K_1,2K_2}^{r,m,3n}\cos(m\phi_\alpha+(3n-m)\phi_\beta) - a_{2K_1,2K_2}^{i,m,3n}\sin(m\phi_\alpha+(3n-m)\phi_\beta)\big]\,. \quad (12)$$

Redundancy occurs when both m and n have their signs flip. To avoid the redundancy, we further constrain $n \geq 0$, and when $n = 0$, $m \geq 0$. Similar constraints on ranges of summation indices are enforced for other cases when the real part is taken.

4.4. Finalizing the vibronic Hamiltonian matrix

Once all unique matrix element expansions are obtained at the desired orders, they may be mapped to all the other elements to complete the vibronic Hamiltonian matrix. The other matrix elements are either identical to the unique matrix elements or related by complex conjugation. Furthermore, whenever applicable, the conversion to matrix elements of the real E component states is carried out. The conversion to the real E component states $|X\rangle$ and $|Y\rangle$ from complex states $|+\rangle$ and $|-\rangle$ is accomplished by unitary transformation of the complex vibronic Hamiltonian matrix $\underline{\underline{H}}^c$, $\underline{\underline{H}}^r = \underline{\underline{U}}\,\underline{\underline{H}}^c\underline{\underline{U}}^\dagger$, where the double-underlines denote matrices, and the the c and r superscripts denote the complex-valued and real-valued matrices. $\underline{\underline{U}}$ is derived from the transformations in Eq. 5. For example of $(E+E)$ type problems, the appropriate unitary matrix is

$$U = \frac{1}{\sqrt{2}} \begin{pmatrix} 1 & 1 & 0 & 0 \\ i & -i & 0 & 0 \\ 0 & 0 & 1 & 1 \\ 0 & 0 & i & -i \end{pmatrix}. \tag{13}$$

Additionally, conversion of e vibrational coordinates from polar to cartesian may be performed. Each term in the matrix element is then fully expanded and simplified to yield succinct expressions in cartesian coordinates. We note that the conversion of high-order terms in polar coordinates, e.g., terms with $\sin m\phi$ or $\cos m\phi$, and a large m, to cartesian coordinates is often the most time-consuming step in running the program. All steps in this subsection are connected by dashed arrows in Figure 1.

4.5. Example: 3rd order expansion for $E' \otimes (e' + a_1'')$ in D_{3h}

The input specifying the third order expansion of vibronic Hamiltonian matrix elements for the $E' \otimes (e' + a_1'')$ JT problem in D_{3h} symmetry is:

$$G_n : D_{3h}, \quad (\Gamma_\alpha + \Gamma_\beta) \otimes (\gamma_\alpha + \gamma_\beta) : E' \otimes (e' + a_1''), \quad \{o_i\} : \{3\}. \tag{14}$$

The program goes through the first three steps in Section 3 to determine there are two unique matrix elements, $H_{+'+'}$ and $H_{+'-'}$. $H_{+'+'}$ takes the following root expansion,

$$\rho^{|3m|+2K}(a^{r,3m}_{I_1,2K} z^{I_1} \cos(3m\phi) - a^{i,3m}_{I_2,2K} z^{I_2} \sin(3m\phi)), \tag{15}$$

with the constraints: (1) only the cosine terms remain; (2) I_1 and I_2 have to be even. Similarly, the root formula of $H_{+'-'}$ is

$$\begin{aligned} \rho^{|3n-1|+2K}[& b^{r,3n-1}_{I_1,2K} z^{I_1} \cos((3n-1)\phi) - b^{i,3n-1}_{I_2,2K} z^{I_2} \sin((3n-1)\phi) \\ & -i(b^{r,3n-1}_{I_1,2K} z^{I_1} \sin((3n-1)\phi)) + b^{i,3n-1}_{I_2,2K} z^{I_2} \cos((3n-1)\phi))], \end{aligned} \tag{16}$$

and the constraints are: (1) only the terms with the b^r coefficients remain; (2) I_1 and I_2 need to be even.

For $H_{+'+'}$ only the $a^{r,3m}_{I_1,2K} z^{I_1} \rho^{|3m|+2K} \cos(3m\phi)$ term in Eq.15 remains because of the "cos nz" constraint. The relevant summation indices are $3m$, I_1, and $2K$. At the third order, this generates summation index value sets $I_1 \in \{0,1,2,3\}$, $2K \in \{0,2\}$, and $3m \in \{0,3\}$. $3m = -3$ is not included since $\chi^{C_2'}_{Im} = 0$ for $H_{+'+'}$ thus m must be non-negative to avoid redundancy. All possible combinations of these summation indices are generated following the enumeration $S_i = (I_1, 2K, 3m)$:

$$
\begin{aligned}
S = \{&(0,0,0),(0,0,3),(0,2,0),(0,2,3),(1,0,0),(1,0,3),(1,2,0),(1,2,3),\\
&(2,0,0),(2,0,3),(2,2,0),(2,2,3),(3,0,0),(3,0,3),(3,2,0),(3,2,3)\}.
\end{aligned}
\tag{17}
$$

For each combination S_i in S, it is checked whether the resulting term (1) is of correct order and (2) satisfies the relevant contraints. The order of a term is defined as the sum over its power arguments, e.g., $I_1 + |3m| + 2K$ for $a^{r,3m}_{I_1,2K} z^{I_1} \rho^{|3m|+2K} \cos(3m\phi)$. Combinations in which $I_1 + |3m| + 2K = 3$ are found to be $(0,0,3)$, and $(1,2,0)$. All others are neglected. Since I_1 and I_2 need to be even, only $S_i = (0,0,3)$ survives. The resulting third order expansion of $H_{+'+'}$ has only one term:

$$
H^{(3)}_{+'+'} = a^{r,3}_{0,0} \rho^3 \cos(3\phi). \tag{18}
$$

The expansion procedure is repeated for $H_{+'-'}$. The terms to be iterated in Eq.16 are:

$$
b^{r,3n-1}_{I_1,2K} z^{I_1} \rho^{|3n-1|+2K} \cos((3n-1)\phi) - i b^{r,3n-1}_{I_1,2K} z^{I_1} \rho^{|3n-1|+2K} \sin((3n-1)\phi). \tag{19}
$$

due to the "b^r nz" constraint. The summation index value sets are generated from $I \in \{0,1,2,3\}$, $2K \in \{0,2\}$, and $3n-1 \in \{-1,2\}$ following the order $(I, 2K, 3n-1)$:

$$
\begin{aligned}
S = \{&(0,0,-1),(0,0,2),(0,2,-1),(0,2,2),(1,0,-1),(1,0,2),(1,2,-1),(1,2,2),\\
&(2,0,-1),(2,0,2),(2,2,-1),(2,2,2),(3,0,-1),(3,0,2),(3,2,-1),(3,2,2)\}.
\end{aligned}
\tag{20}
$$

The order of the terms in $H_{+'-'}$ is $I + |3n-1| + 2K$. Combinations in S which yield third order terms are found to be $(0,2,-1)$, $(1,0,2)$, and $(2,0,-1)$. All terms in the expansion are subject to the constraint "I even", which removes $S_i = (1, 0, 2)$ from the order-satisfying subset of S. The resulting expansion for $H_{+'-'}$ is obtained:

$$\begin{aligned} H^{(3)}_{+'-'} =& ib^r_{0,2,-1}\rho^3 \sin(\phi) + b^r_{0,2,-1}\rho^3 \cos(\phi) \\ & - ib^r_{2,0,-1}z^2\rho \sin(\phi) + b^r_{2,0,-1}z^2\rho \cos(\phi). \end{aligned} \tag{21}$$

The final step to obtaining the complete vibronic Hamiltonian is to map the unique matrix element expansions to all the other elements. From the time-reversal symmetry and hermiticity of the operator, $H_{-'-'} = H_{+'+'}$, and $H_{-'+'} = H^*_{+'-'}$. The obtained third order JT Hamiltonian in product matrix form reads:

$$\hat{H} = \begin{pmatrix} |+'\rangle & |-'\rangle \end{pmatrix} \begin{pmatrix} a^{r,3}_{0,0}\rho^3 \cos(3\phi) & \begin{matrix} ib^r_{0,2,-1}\rho^3 \sin(\phi) + b^r_{0,2,-1}\rho^3 \cos(\phi) \\ -ib^r_{2,0,-1}z^2\rho \sin(\phi) + b^r_{2,0,-1}z^2\rho \cos(\phi) \end{matrix} \\ c.c & a^{r,3}_{0,0}\rho^3 \cos(3\phi) \end{pmatrix} \begin{pmatrix} \langle +'| \\ \langle -'| \end{pmatrix}, \tag{22}$$

where $c.c$ denotes complex conjugation of the off-diagonal element. The resultant vibronic Hamiltonian may be readily transformed to the real E basis with the $|X'\rangle$ and $|Y'\rangle$ components. The transformation matrix is just the first 2×2 diagonal block matrix in Eq. 13. Additionally, the matrix elements may be converted from polar coordinates to cartesian coordinates. The vibronic Hamiltonians generated by `VHEGEN` are correct, complete, and primed for fitting of expansion coefficents for implementation in vibronic simulations.

5. Practical aspects of `VHEGEN`

Within this section, installation and application of the package are described along with its general capabilities. We first review the dependencies of the program and its installation procedure. Following, the use of the `VHEGEN` package as a blackbox procedural program is discussed. Finally, we provide an in-depth description of various methods and attributes of the `VHEGEN` class, accessed by importing the package as a Python module.

5.1. Installing `VHEGEN`

`VHEGEN` is compatible with Python 2/3 on Linux, Windows, and MacOS, and depends on external Python libraries Sympy and Numpy [63, 64]. The straightforward installation outlined herein will prime the program for procedural use as an executable script, as well as for importing as a Python package local to the installation directory. Installation of the `VHEGEN` package begins with uncompressing the package `.zip` file to the user's preferred write-allowed directory. If `pip` is installed, one can quickly obtain the required external library dependencies by executing

```
$ pip install -r requirements.txt
```

in the main directory. This will automatically install/update Sympy, Numpy, and any other missing Python libraries to the machine. Otherwise, these modules may be easily obtained and built from source. It is recommended to test that the package and all external dependencies are properly installed by entering the Python interactive shell in the main directory and attempting to import the `vhegen` module.

```
>>> import vhegen
```

If no `ImportError` is raised, all dependencies are installed and `VHEGEN` is ready to be used. It is also recommended the system has a TeX distribution with `pdflatex` functionality installed, such as TeX Live. This will allow the user to obtain the final matrix element expansions typeset via LaTeX in an output PDF file. This feature significantly enhances the output vibronic Hamiltonian's readability.

5.2. Using `VHEGEN` procedurally

Procedural usage of the package offers a blackbox approach to obtaining specific vibronic Hamiltonian matrix element expansions. An overview of the procedural output formats available are described in Section 5.2.5. `VHEGEN` is called procedurally by executing command

```
$ python vhegen.py
```

in the main directory. The programs settings for procedural use are read from the configuration file `config.cfg` in the same directory. This file contains various configurational parameters discussed below. Within the remainder of this subsection, we describe how to configure `VHEGEN` for procedural use in detail, the static and dynamic input methods, and obtaining the final output vibronic Hamiltonian.

5.2.1. Configuration

In the configuration file for `VHEGEN`, `config.cfg`, the user specifies the five parameters: `input`, `pdf_out`, `log_out`, `e_coords`, and `basis`.

```
#VHEGEN program example configuration
input = dynamic
pdf_out=true
log_out=true
e_coords=pol
basis=real
```

The allowed values for the configurational parameters are summarized in Table 6.

Config. parameter	Values
`input`	`static`, `dynamic`
`pdf_out`	`true`, `false`
`log_out`	`true`, `false`
`e_coords`	`cart`, `pol`, `both`
`basis`	`complex`, `real`, `both`

Table 6: Parameters required in `VHEGEN` configuration file and their allowed values.

Parameter `input` is used to specify either the static or the dynamic input mode (Section 5.2.2). When set to `true`(`false`), parameter `pdf_out` enables(disables) application of the TeX `pdflatex` command to produce a PDF output file. The output file contains the input vibronic interaction, the form of the vibronic Hamiltonian matrix, and all explicit matrix element expansions typeset via LaTeX. Thus, `pdf_out` should only be set to `true` if a TeX distribution is installed on the system. Parameter `log_out` similarly enables or disables output of a text file, containing all relevant information used in the expansion process, including: the unique matrix elements and their symmetry eigenvalues, and the root expansion formulas along with their constraints. All expansions can also be found in the `log` file, however in Sympy readable syntax. Parameter `e_coords` is used to specify the coordinate system used for expressing e-type vibrational modes. When `e_coords` is set to `pol`, the expansions will be kept in polar coordinates as they were originally constructed. When `e_coords` is set to `cart`, the expansions are converted to cartesian coordinates by coordinate transformation described in Section 4.4. Both polar and cartesian coordinate expansions may be included in the final output by setting `e_coords=both`. The `basis` parameter defines which basis to use for vibronic Hamiltonians involving E-type electronic states. When set to `complex`, the output vibronic Hamiltonian matrix elements are for the complex E component states $|+\rangle$ and $|-\rangle$. Alternatively, when `basis` is set to `real`, the output Hamiltonian matrix is for the real E component states $|X\rangle$ and $|Y\rangle$. Both complex and real representations can be output by setting `basis=both`.

5.2.2. Input

The procedural input to `VHEGEN` consists of specifying: point group symmetry, irreps of electronic states, irreps of vibrational modes, order(s) of expansion, and an output filename. There exist two input approaches, namely the "dynamic input" and "static input" modes, selected using the `input` configuration parameter.

Both modes of input follow the same general rules for input syntax. All input parameters are case-insensitive, except the output filename. Symmetries are specified by their usual point group classification. Electronic states and vibrational modes are specified by standard Mulliken symbols for their irreps. Single primes in Mulliken symbols are denoted by an apostrophe `'`, and double primes are denoted by two apostrophes `''` or a quotation mark `"`. For pJT problems that involve two states or bimodal problems that involve two vibrational modes, either a plus sign `+` or a comma `,` can be used to separate the two specified states or modes. When specifying the orders of expansion, a range of orders can be stated by providing non-negative integers as lower and upper inclusive bounds separated by a comma, e.g., `0,6`. If expansion at a single order is desired, then only an integer is keyed in. Output filename should avoid any (operating system dependent) illegal characters. If the filename parameter is unspecified or left empty, the output filename will default to value `output`.

5.2.3. Dynamic input

When dynamic input mode is specified in the configuration file, the user enters problem parameters and output filename dynamically through terminal prompts after executing command `python vhegen.py`. Any additional arguments made when calling the program will be ignored if set to dynamic input. The user will be re-prompted at each stage if an invalid parameter is entered.

Below is an example of procedurally calling `VHEGEN` in dynamic input mode, for specification of the 3rd to 6th order expansion of Hamiltonian matrix elements for the $E \otimes (e + a_1)$ JT interaction in C_{3v} symmetry.

```
Entering dynamic input.
Enter symmetry: C3V
```

```
C3V symmetry accepted.
Enter electronic state(s): E
Electronic states (E) accepted.
Enter vibrational mode(s): E+A1
Vibrational modes (e+a1) accepted.
Order(s) of expansion:3,6
Orders of expansion [3, 4, 5, 6] accepted.
Enter filename: output
Filename: ``output''.
```

5.2.4. Static input

When input mode is set to static, a vibronic problem is specified in-line with the execution of the program via additional arguments. The following additional arguments must be specified in the static input mode: "`sym`" for point group symmetry, "`states`" for electronic state(s), "`modes`" for vibrational mode(s), and "`o`" for order(s) of expansion. Specification of a filename is done by argument "`f`". The general syntax for specifying the additional arguments when executing the program is "`--arg=value`". For example, the input of the same $E \otimes (e + a_1)$ problem in static mode is:

```
$ python vhegen.py --sym=C3V --states=E --modes=e+a1 --o=3,6
```

5.2.5. Output

When called procedurally, `VHEGEN` produces up to three output files. These files will be generated in subdirectory `outputs`, within the package directory. These files are the output `.log` file (if `log_out=true`), the output `.tex` file, which is compiled by executing `pdflatex` to generate the output `.pdf` file (if `pdf_out=true`). The `.log` file is a text file containing the unique matrix elements' symmetry eigenvalues, as well as all matrix elements' expansions for all specified orders in their Sympy expression syntax. The `.tex` file is a TeX input file containing the general matrix form of the vibronic problem, and all matrix element expansions for all orders specified, typeset via LaTeX format.

5.3. Using `VHEGEN` as a package

One may wish to use `VHEGEN` as an importable package rather than calling it procedurally from terminal. This allows for the utilization of the `VHEGEN` class in user's Python scripts, enabling further application of the obtained vibronic Hamiltonian. While the design philosophy of `VHEGEN` has an emphasis on the streamline between input and user-friendly output when called procedurally, using it as a package enables additional functionality. Methods in the `VHEGEN` class are fully accessible when used as a module, making all information available to the user by convenient datastructures. This significantly enhances the scope of applications to the program. Herein we describe the various methods and attributes included in the `VHEGEN` class.

5.3.1. Initialization

To initialize an instance of the `VHEGEN` class, a dictionary containing all vibronic problem parameters for that instance must be specified as its only argument. To avoid complications with syntax, it is recommended to use the `prepare_input()` function from the `input` module. `prepare_input()` takes five arguments: point group symmetry, the electronic states, the vibrational modes, order(s) of expansion, and an optional filename. All arguments are given as strings, following the same syntax used for the procedural input process. For example, initializing an instance of `VHEGEN` for the $(E + A) \otimes (e + a)$ problem in C_4 symmetry with expansion at the 12th order is shown below.

```
import vhegen as vhe

params = vhe.inp.prepare_input(sym='C4',
                               states='E+A',
                               modes='e+a',
                               orders='12',
                               filename='output')

vhegen_instance = vhe.VHEGEN(params)
```

The input attributes of the initialized instance can be checked by printing them to console by the `return_init()` method. Alternatively, they can be accessed directly. Symmetry of the problem, electronic states, vibrational modes, and orders of expansion are stored in class attributes `symmetry`, `states`, `modes`, and `orders`, respectively. If the `VHEGEN` instance is initialized with a vibronic problem involving e-type vibrational modes, the e coordinate system is set to polar by default. If one wishes to switch to cartesian coordinates, or have expansions generated in both coordinate systems, this is accomplished by the `set_e_coordinates()` method, which takes `'cart'`, `'pol'`, or `'both'` as allowed arguments. The setting of desired coordinates must be done before beginning the expansion process. Similarly, one can change basis of E electronic states from complex using `set_basis`, which takes `'real'`, `'complex'`, or `'both'` as its argument. A `VHEGEN` class instance is initialized with e coordinates and E basis set to `'both'` by default.

5.3.2. Generating matrix element expansions

After initialization of a `VHEGEN` instance, the matrix product form of the vibronic Hamiltonian, the unique matrix elements, and their symmetry eigenvalues are obtained by `init_matrix_form()`, which initializes attributes `matrix` and `eigenvals`. Attribute `eigenvals` is a dictionary with keys being the unique matrix elements in the complex basis, and values being a list of its symmetry eigenvalues. The lists of eigenvalues follow the same enumeration as used throughout this paper.

$$\texttt{eigenvals} = \left\{ H^{\circ}_{ij} : \left[\chi^{C_n}, \left(\chi^{\sigma_v/C_2'}_{Re}, \chi^{\sigma_v/C_2'}_{Im} \right), \chi^{I/\sigma_h}_{H_{ij}} \right] \right\} \tag{23}$$

Once the eigenvalues of the unique matrix elements are known, i.e., attribute `eigenvals` has been initialized, `VHEGEN` has all information necessary to select the unique matrix elements' root expansion formulas and constraints. Method `get_formulas()` performs the lookup of root expansion formulas for the unique matrix elements in `eigenvals` and stores them in attribute `formulas`. Method `get_formulas()` also calls `get_constraints()`, performing the search for constraints in the appropriate `.sym` constraint file(s) in the `constraints` directory, storing them in attribute `constraints`. Expansion of the unique matrix elements is carried out by method `get_expansions()`, storing them in attribute `expansions`. The data structure for `expansions` is a nested dictionary:

$$\texttt{expansions} = \{o_i : \{H_{ij} : H^{(o_i)}_{ij}\}\} \tag{24}$$

The outer dictionary's keys correspond to the orders of expansion o_i. The values correspond to inner dictionaries, each of which has keys holding the vibronic Hamiltonian matrix elements $\{H_{ij}\}$, and their values corresponding to their expansions in vibrational coordinates at the specific order for which the dictionary is associated with. $H^{(o_i)}_{ij}$ is a two-element list if the e coordinates have been set to `both`, storing the expansions in polar followed by cartesian. Otherwise, list $H^{(o_i)}_{ij}$ has only one element. The matrix element expansions are Sympy expressions, and can be manipulated as such. In converting the Hamiltonian matrix from the complex to the real E basis, the unitary transformation is done by method `basis_transformation()`. If the E basis has been set to `both`, expansions for the real basis elements are stored in separate attribute `expansions_real` with the same data structure as Eq. 24.

5.3.3. The ***auto()*** *method*

All the aforementioned methods are called internally when `VHEGEN` is run procedurally. Due to the importance of these operations, we implemented a simplified method named `auto()`. The `auto()` method can be called directly after initialization of the `VHEGEN` instance, and it automatically calls all mandatory processes discussed above to generate the `expansions` attribute including all matrix elements. It will automatically transform to the real E component basis if applicable. Below is an example Python script of how one would concisely generate the expanded matrix elements for a specific vibronic Hamiltonian at the desired orders of expansion through inporting `VHEGEN`.

```
import vhegen as vhe

params = vhe.inp.prepare_input(sym='D4h',
                               states='Eg+A1u',
                               modes='eg+b2u',
                               orders='0,10')

vhegen_instance = vhe.VHEGEN(params)
vhegen_instance.auto()
print(vhegen_instance.expansions)
```

The `VHEGEN` instance after `auto()` has all other properties intermediate to the input parameters and output expansions, which can be referenced by the usual attribute names.

6. Benchmarking

Within this section, we demonstrate the validity of `VHEGEN` by comparing the expansions generated by the code with previously reported formulas. We first choose the well-studied $(E' + A_2'') \otimes (e' + a_2'')$ problem in D_{3h} symmetry, for which Bhattacharyya et al. provide explicit expansions for all intraterm and interterm vibronic matrix elements in Ref. 33. Please note that the conventional $(E' + A_2'') \otimes (e' + a_2'')$ vibronic interaction includes, in our notations, the $E' \otimes (e' + a_2'')$ intra-term coupling, the $A_2'' \otimes (e' + a_2'')$ intra-term coupling, and the $(E' + A_2'') \otimes (e' + a_2'')$ inter-term coupling. In Ref. 33, the matrix element expansions were obtained up to the eighth order by employing the Weyl's polarization method and the polynomial invariant theory [65, 66, 67]. It provides a useful benchmark to gauge the correctness of VHEGEN. All six unique matrix elements in the three-state vibronic matrix may be produced by running VHEGEN with the three intra- and inter-term input problems: $E' \otimes (e' + a_2'')$ for H_{XX}, H_{XY}, and H_{YY}, $A_2'' \otimes (e' + a_2'')$ for H_{AA}, and $(E' + A_2'') \otimes (e' + a_2'')$ for H_{XA} and H_{YA}. The matrix element expansions up to the fifth order are shown below.

$$\begin{aligned}
H_{AA}^{(0\text{-}5)} &= a^r_{0,0,0} + a^r_{0,2,0}\left(x^2+y^2\right) + a^r_{2,0,0}z^2 + a^r_{0,0,3}x\left(x^2-3y^2\right) + a^r_{0,4,0}\left(x^2+y^2\right)^2 \\
&\quad + a^r_{2,2,0}z^2\left(x^2+y^2\right) + a^r_{4,0,0}z^4 + a^r_{0,2,3}x\left(x^2-3y^2\right)\left(x^2+y^2\right) \\
&\quad + a^r_{2,0,3}xz^2\left(x^2-3y^2\right) \qquad (25)
\end{aligned}$$

$$\begin{aligned}
H_{XA}^{(0\text{-}5)} &= \sqrt{2}b^r_{1,0,-1}xz + \sqrt{2}b^r_{1,0,2}z\left(x^2-y^2\right) + \sqrt{2}\left(b^r_{1,2,-1}xz\left(x^2+y^2\right) + b^r_{3,0,-1}xz^3\right) \\
&\quad + \sqrt{2}\Big(b^r_{1,0,-4}z\left(x^4-6x^2y^2+y^4\right) + b^r_{1,2,2}z\left(x^4-y^4\right) \\
&\quad + b^r_{3,0,2}z^3\left(x^2-y^2\right)\Big) \qquad (26)
\end{aligned}$$

$$\begin{aligned}
H_{YA}^{(0\text{-}5)} &= \sqrt{2}b^r_{1,0,-1}yz - 2\sqrt{2}b^r_{1,0,2}xyz - \sqrt{2}\left(-b^r_{1,2,-1}yz\left(x^2+y^2\right) - b^r_{3,0,-1}yz^3\right) \\
&\quad - \sqrt{2}\left(-4b^r_{1,0,-4}xyz\left(x^2-y^2\right) + 2b^r_{1,2,2}xyz\left(x^2+y^2\right) + 2b^r_{3,0,2}xyz^3\right) \qquad (27)
\end{aligned}$$

$$\begin{aligned}
H_{XX}^{(0\text{-}5)} &= a^r_{0,0,0} + b^r_{0,0,-1}x + a^r_{0,2,0}\left(x^2+y^2\right) + a^r_{2,0,0}z^2 + b^r_{0,0,2}\left(x^2-y^2\right) + a^r_{0,0,3}x\left(x^2-3y^2\right) \\
&\quad + b^r_{0,2,-1}x\left(x^2+y^2\right) + b^r_{2,0,-1}xz^2 + a^r_{0,4,0}\left(x^2+y^2\right)^2 + a^r_{2,2,0}z^2\left(x^2+y^2\right) + a^r_{4,0,0}z^4 \\
&\quad + b^r_{0,0,-4}\left(x^4-6x^2y^2+y^4\right) + b^r_{0,2,2}\left(x^4-y^4\right) + b^r_{2,0,2}z^2\left(x^2-y^2\right) \\
&\quad + a^r_{0,2,3}x\left(x^2-3y^2\right)\left(x^2+y^2\right) + a^r_{2,0,3}xz^2\left(x^2-3y^2\right) + b^r_{0,0,5}x\left(x^4-10x^2y^2+5y^4\right) \\
&\quad + b^r_{0,4,-1}x\left(x^2+y^2\right)^2 + b^r_{2,2,-1}xz^2\left(x^2+y^2\right) + b^r_{4,0,-1}xz^4 \qquad (28)
\end{aligned}$$

$$\begin{aligned}
H_{YY}^{(0\text{-}5)} &= a^r_{0,0,0} - b^r_{0,0,-1}x + a^r_{0,2,0}\left(x^2+y^2\right) + a^r_{2,0,0}z^2 - b^r_{0,0,2}\left(x^2-y^2\right) + a^r_{0,0,3}x\left(x^2-3y^2\right) \\
&\quad - b^r_{0,2,-1}x\left(x^2+y^2\right) - b^r_{2,0,-1}xz^2 + a^r_{0,4,0}\left(x^2+y^2\right)^2 + a^r_{2,2,0}z^2\left(x^2+y^2\right) + a^r_{4,0,0}z^4 \\
&\quad - b^r_{0,0,-4}\left(x^4-6x^2y^2+y^4\right) - b^r_{0,2,2}\left(x^4-y^4\right) - b^r_{2,0,2}z^2\left(x^2-y^2\right) \\
&\quad + a^r_{0,2,3}x\left(x^2-3y^2\right)\left(x^2+y^2\right) + a^r_{2,0,3}xz^2\left(x^2-3y^2\right) - b^r_{0,0,5}x\left(x^4-10x^2y^2+5y^4\right) \\
&\quad - b^r_{0,4,-1}x\left(x^2+y^2\right)^2 - b^r_{2,2,-1}xz^2\left(x^2+y^2\right) - b^r_{4,0,-1}xz^4 \qquad (29)
\end{aligned}$$

$$\begin{aligned}
H_{XY}^{(0\text{-}5)} &= b^r_{0,0,-1}y - 2b^r_{0,0,2}xy + b^r_{0,2,-1}y\left(x^2+y^2\right) + b^r_{2,0,-1}yz^2 + 4b^r_{0,0,-4}xy\left(x^2-y^2\right) \\
&\quad - 2b^r_{0,2,2}xy\left(x^2+y^2\right) - 2b^r_{2,0,2}xyz^2 - b^r_{0,0,5}y\left(5x^4-10x^2y^2+y^4\right) + b^r_{0,4,-1}y\left(x^2+y^2\right)^2 \\
&\quad + b^r_{2,2,-1}yz^2\left(x^2+y^2\right) + b^r_{4,0,-1}yz^4 \qquad (30)
\end{aligned}$$

Please note that the numerical values of the a^r coefficients in H_{XX} and H_{YY} are different from those in H_{AA}, and the numerical values of the b^r

coefficients in H_{XX}, H_{YY}, and H_{XY} are different from those in H_{XA} and H_{YA}. The expansions generated by VHEGEN are in perfect agreement with those reported in Ref. 33, except for the trivial $\sqrt{2}$ factor, which is introduced in the complex-to-real E bases transformation, and some trivial recombinations of terms.

We also compare the VHEGEN-generated expansions up to 6th order for the $E'' \otimes (e' + e')$ intra-term coupling matrix elements with those reported in Ref. 28. To maintain a readable length of this article, we do not show the expansions here. The PDF output of this VHEGEN run is included as the second supplementary file, with the filename VHE_testrun.pdf. The produced expansions of the H_{XX}, H_{YY}, and H_{XY} elements are seen in Section 5 of the this file. They are again in perfect agreement with those reported in Ref. 28. The agreements in the two comparisons clearly demonstrate the robustness of the program.

7. Conclusions and future work

In this paper we present VHEGEN, a Python package capable of generating expansion formulas for all bimodal JT/pJT Hamiltonian matrix elements in trigonal and tetragonal symmetries. The expansions can be up to arbitrarily high order in vibrational coordinates. Prior to this work, it may take days or even weeks to derive expansion formulas for a JT/pJT Hamiltonian of interest. The use of VHEGEN reduces all these efforts to a matter of minutes. And all we need to specify is the JT/pJT problem and the range of orders. The program generates the order-by-order, term-by-term expansion formulas, which are correct, complete, and concise. The VHEGEN package presents itself as a powerful tool for future JT/pJT studies.

The highly generalized nature of the applied formalism, and correspondingly the program implementation, facilitate the enhancement of the problem scope to other symmetries for future versions. The systematic problem-to-eigenvalue reduction, the root-branch approach, and the modularized approach, which have been employed to handle the trigonal and tetragonal symmetries, pave the way to general expansion formulas for problems in arbitrary axial symmetries, i.e., the C_n, S_n, C_{nh}, C_{nv}, D_n, D_{nd}, and D_{nh} symmetries with arbitrary n (note that S_n only exists for even n). Once derived, the general axial formalism can be readily incorporated to the program. Further, we have recently derived all unimodal and bimodal JT/pJT formalisms in tetrahedral and octahedral symmetries. These formalisms will also be incorporated in the future version of the program.

8. Acknowledgements

T. Z. thanks York University (481333), Carleton University (186853), and the Natural Sciences and Engineering Research Council (NSERC) of Canada for funding (RGPIN-2016-06276). R. J. H. acknowledges NSERC for provision of the Postgraduate Scholarships-Doctoral Program (PGSD3-534584-2019).

[1] M. Born and R. Oppenheimer, "Zur quantentheorie der molekeln," *Annalen der Physik*, vol. 389, no. 20, pp. 457–484, 1927.

[2] M. Born and K. Huang, *Dynamical Theory of Crystal Lattices.* Oxford, England, UK: Oxford University Press, 1954.

[3] D. R. Yarkony, "Nonadiabatic quantum chemistry—past, present, and future," *Chemical Reviews*, vol. 112, pp. 481–498, jan 2012.

[4] B. E. Applegate, T. A. Barckholtz, and T. A. Miller, "Explorations of conical intersections and their ramifications for chemistry through the Jahn–Teller effect," *Chem. Soc. Rev.*, vol. 32, no. 1, pp. 38–49, 2003.

[5] I. B. Bersuker, "A unique Jahn–Teller mechanism of all the symmetry breakings in molecular systems and condensed matter," in *Advances in Quantum Chemistry*, vol. 44 of *Advances in Quantum Chemistry*, pp. 1 – 12, Academic Press, 2003.

[6] I. Bersuker, *The Jahn-Teller-Effect and vibronic interactions in modern chemistry.* Modern Inorganic Chemistry Series, Plenum Publishing Company Limited, 1984.

[7] W. Domcke and D. R. Yarkony, "Role of conical intersections in molecular spectroscopy and photoinduced chemical dynamics," *Annual Review of Physical Chemistry*, vol. 63, no. 1, pp. 325–352, 2012. PMID: 22475338.

[8] I. B. Bersuker, "Pseudo-Jahn–Teller effect—a two-state paradigm in formation, deformation, and transformation of molecular systems and solids," *Chemical Reviews*, vol. 113, no. 3, pp. 1351–1390, 2013. PMID: 23301718.

[9] M. A. Halcrow, "Jahn–Teller distortions in transition metal compounds, and their importance in functional molecular and inorganic materials," *Chem. Soc. Rev.*, vol. 42, no. 4, pp. 1784–1795, 2013.

[10] J. B. Goodenough, "Jahn-Teller phenomena in solids," *Annual Review of Materials Science*, vol. 28, no. 1, pp. 1–27, 1998.

[11] T. A. Barckholtz, "Quantitative insights about molecules exhibiting Jahn-Teller and related effects," *International Reviews in Physical Chemistry*, vol. 17, pp. 435–524, oct 1998.

[12] I. B. Bersuker, “Modern aspects of the Jahn−Teller effect theory and applications to molecular problems,” *Chemical Reviews*, vol. 101, no. 4, pp. 1067–1114, 2001. PMID: 11709858.

[13] J. C. Tully, “Perspective: Nonadiabatic dynamics theory,” *The Journal of Chemical Physics*, vol. 137, no. 22, p. 22A301, 2012.

[14] B. F. E. Curchod and T. J. Martínez, “Ab initio nonadiabatic quantum molecular dynamics,” *Chemical Reviews*, vol. 118, no. 7, pp. 3305–3336, 2018. PMID: 29465231.

[15] H. Köppel, “Diabatic representation: Methods for the conctruction of diabatic electronic states,” in *Conical Intersections: Electronic Structure, Dynamics & Spectroscopy*, pp. 175–204, World Scientific Publishing, jul 2004.

[16] W. Domcke, D. Yarkony, and H. Köppel, *Conical Intersections: Theory, Computation and Experiment*. Advanced series in physical chemistry, World Scientific Publishing Company, 2011.

[17] H. A. Jahn and E. Teller, “Stability of polyatomic molecules in degenerate electronic states. I. orbital degeneracy,” *Proceedings of the Royal Society A: Mathematical, Physical and Engineering Sciences*, vol. 161, pp. 220–235, jul 1937.

[18] U. Opik and M. H. L. Pryce, “Studies of the Jahn-Teller effect. I. a survey of the static problem,” *Proceedings of the Royal Society A: Mathematical, Physical and Engineering Sciences*, vol. 238, pp. 425–447, jan 1957.

[19] I. B. Bersuker, *The Jahn-Teller Effect*. Cambridge, UK: Cambridge University Press, 2006.

[20] T. Zeng, D. G. Fedorov, M. W. Schmidt, and M. Klobukowski, “Effects of spin–orbit coupling on covalent bonding and the Jahn–Teller effect are revealed with the natural language of spinors,” *Journal of Chemical Theory and Computation*, vol. 7, no. 9, pp. 2864–2875, 2011. PMID: 26605477.

[21] T. Zeng, D. G. Fedorov, M. W. Schmidt, and M. Klobukowski, “Natural spinors reveal how the spin–orbit coupling affects the Jahn–Teller

distortions in the hexafluorotungstate(V) anion," *Journal of Chemical Theory and Computation*, vol. 8, no. 9, pp. 3061–3071, 2012. PMID: 26605717.

[22] T. Pacher, L. S. Cederbaum, and H. Köppel, "Approximately diabatic states from block diagonalization of the electronic Hamiltonian," *The Journal of Chemical Physics*, vol. 89, pp. 7367–7381, dec 1988.

[23] H. Köppel, J. Gronki, and S. Mahapatra, "Construction scheme for regularized diabatic states," *The Journal of Chemical Physics*, vol. 115, pp. 2377–2388, aug 2001.

[24] T. Pacher, L. S. Cederbaum, and H. Köppel, "Adiabatic and quasidiabatic states in a gauge theoretical framework," in *Advances in Chemical Physics*, pp. 293–391, Wiley, mar 2007.

[25] T. Zeng, "A diabatization protocol that includes spin-orbit coupling," *The Journal of Chemical Physics*, vol. 146, no. 14, p. 144103, 2017.

[26] R. J. Cave and J. F. Stanton, "A simple quasi-diabatization scheme suitable for spectroscopic problems based on one-electron properties of interacting states," *The Journal of Chemical Physics*, vol. 144, no. 5, p. 054110, 2016.

[27] V. Z. Bersuker, I. B.; Polinger, *Vibronic Interactions in Molecules and Crystals*. Springer-Verlag Berlin, 1989.

[28] W. Eisfeld, O. Vieuxmaire, and A. Viel, "Full-dimensional diabatic potential energy surfaces including dissociation: The ${}^2E''$ state of NO_3," *The Journal of Chemical Physics*, vol. 140, p. 224109, jun 2014.

[29] A. Viel and W. Eisfeld, "Effects of higher order Jahn-Teller coupling on the nuclear dynamics," *The Journal of Chemical Physics*, vol. 120, pp. 4603–4613, mar 2004.

[30] W. Eisfeld and A. Viel, "Higher order $(A + E) \otimes e$ pseudo-Jahn–Teller coupling," *The Journal of Chemical Physics*, vol. 122, p. 204317, may 2005.

[31] P. Mondal, D. Opalka, L. V. Poluyanov, and W. Domcke, "Ab initio study of dynamical $E \otimes e$ Jahn-Teller and spin-orbit coupling effects in

the transition-metal trifluorides TiF_3 , CrF_3 , and NiF_3," *The Journal of Chemical Physics*, vol. 136, p. 084308, feb 2012.

[32] P. Mondal, D. Opalka, L. V. Poluyanov, and W. Domcke, "Jahn–Teller and spin–orbit coupling effects in transition-metal trifluorides," *Chemical Physics*, vol. 387, pp. 56–65, aug 2011.

[33] S. Bhattacharyya, D. Opalka, L. V. Poluyanov, and W. Domcke, "The $(E + A) \otimes (e + a)$ Jahn–Teller and pseudo-Jahn–Teller Hamiltonian including spin–orbit coupling for trigonal systems," *The Journal of Physical Chemistry A*, vol. 118, pp. 11962–11970, dec 2014.

[34] S. Bhattacharyya, Z. Dai, and W. Domcke, "Quantum dynamics on a three-sheeted six-dimensional ab initio potential-energy surface of the phosphine cation: Simulation of the photoelectron spectrum and the ultrafast radiationless decay dynamics," *The Journal of Chemical Physics*, vol. 143, p. 194301, nov 2015.

[35] A. Weaver, D. W. Arnold, S. E. Bradforth, and D. M. Neumark, "Examination of the $^2A_2'$ and $^2E'$ states of NO_3 by ultraviolet photoelectron spectroscopy of NO_3^-," *The Journal of Chemical Physics*, vol. 94, pp. 1740–1751, feb 1991.

[36] S. Faraji, H. Köppel, W. Eisfeld, and S. Mahapatra, "Towards a higher-order description of Jahn–Teller coupling effects in molecular spectroscopy: The state of NO_3," *Chemical Physics*, vol. 347, pp. 110–119, may 2008.

[37] S. Bhattacharyya, D. Opalka, L. V. Poluyanov, and W. Domcke, "Jahn-Teller theory beyond the standard model," *Journal of Physics: Conference Series*, vol. 428, p. 012015, apr 2013.

[38] Z. Shao, H. Li, S. Zhang, J. Li, Z. Dai, Y. Mo, Y. J. Bae, and M. S. Kim, "The Jahn-Teller effect in $CH_3Cl^+(\tilde{X}E_2)$: A combined high-resolution experimental measurement and ab initio theoretical study," *The Journal of Chemical Physics*, vol. 136, p. 064308, feb 2012.

[39] T. Mondal, "On the higher-order $T_2 \otimes (e + t_2)$ Jahn–Teller coupling effects in the photodetachment spectrum of the alanate anion (AlH_4^-)," *Phys. Chem. Chem. Phys.*, vol. 20, pp. 9401–9410, 2018.

[40] S. Sen and T. Mondal, “The Jahn–Teller effect in the ground electronic state of the tetrafluoromethane cation before dissociation: a promoter of the anisotropic fragmentation,” *Molecular Physics*, vol. 0, no. 0, pp. 1–13, 2019.

[41] T. Codd, M.-W. Chen, M. Roudjane, J. F. Stanton, and T. A. Miller, “Jet cooled cavity ringdown spectroscopy of the $A\ {}^2E'' \longleftarrow X\ {}^2A_2'$ transition of the NO_3 radical,” *The Journal of Chemical Physics*, vol. 142, p. 184305, may 2015.

[42] H. K. Tran, J. F. Stanton, and T. A. Miller, “Quantifying the effects of higher order coupling terms on fits using a second order Jahn-Teller Hamiltonian,” *Journal of Molecular Spectroscopy*, vol. 343, pp. 102 – 115, 2018. Spectroscopy of Large Amplitude Vibrational Motion, on the Occasion of Jon Hougen’s 80th Birthday – Part II.

[43] T. Zeng and I. Seidu, “Revisiting the $(E + A) \otimes (e + a)$ problems of polyatomic systems with trigonal symmetry: general expansions of their vibronic Hamiltonians,” *Physical Chemistry Chemical Physics*, vol. 19, no. 18, pp. 11098–11110, 2017.

[44] R. J. Hickman, R. A. Lang, and T. Zeng, “General formalism for vibronic Hamiltonians in tetragonal symmetry and beyond,” *Physical Chemistry Chemical Physics*, vol. 20, no. 17, pp. 12312–12322, 2018.

[45] T. Zeng, R. J. Hickman, A. Kadri, and I. Seidu, “General formalism of vibronic Hamiltonians for tetrahedral and octahedral systems: Problems that involve T , E states and t, e vibrations,” *Journal of Chemical Theory and Computation*, vol. 13, pp. 5004–5018, oct 2017.

[46] R. A. Lang, A. Japahuge, and T. Zeng, “General formalism of vibronic Hamiltonians for tetrahedral and octahedral systems: Problems that involve A-type states and a-type vibrations,” *Chemical Physics*, vol. 515, pp. 36–45, 2018.

[47] I. Seidu, P. Goel, X.-G. Wang, B. Chen, X.-B. Wang, and T. Zeng, “Vibronic interaction in CO_3- photo-detachment: Jahn–Teller effects beyond structural distortion and general formalisms for vibronic Hamiltonians in trigonal symmetries,” *Phys. Chem. Chem. Phys.*, vol. 21, pp. 8679–8690, 2019.

[48] K. Wang and T. Zeng, "Hamiltonian formalism of spin-orbit Jahn-Teller and pseudo-Jahn-Teller problems in trigonal and tetragonal symmetries," *Phys. Chem. Chem. Phys.*, DOI: 10.1039/C9CP03584B, 2019.

[49] E. P. Winger, *Group Theory.* Academic Press, Inc., 1959.

[50] J. S. Griffith, *The Irreducible Tensor Method for Molecular Symmetry Group.* Dover Publications, Inc., 2006.

[51] A. D. Liehr, "Topological aspects of the conformational stability problem. part II. non-degenerate electronic states 1," *The Journal of Physical Chemistry*, vol. 67, pp. 471–494, feb 1963.

[52] A. Markmann, G. A. Worth, and L. S. Cederbaum, "Allene and pentatetraene cations as models for intramolecular charge transfer: Vibronic coupling Hamiltonian and conical intersections," *The Journal of Chemical Physics*, vol. 122, p. 144320, apr 2005.

[53] A. M. Schulenburg and F. Merkt, "Rotationally resolved photoelectron spectroscopic study of the Jahn–Teller effect in allene," *The Journal of Chemical Physics*, vol. 130, p. 034308, jan 2009.

[54] Y. Liu, I. B. Bersuker, P. Garcia-Fernandez, and J. E. Boggs, "Pseudo Jahn–Teller origin of nonplanarity and rectangular-ring structure of tetrafluorocyclobutadiene," *The Journal of Physical Chemistry A*, vol. 116, pp. 7564–7570, jul 2012.

[55] Y. Liu, Y. Wang, and I. B. Bersuker, "Geometry, electronic structure, and pseudo Jahn-Teller effect in tetrasilacyclobutadiene analogues," *Scientific Reports*, vol. 6, p. 23315, sep 2016.

[56] S. Mahapatra, V. Vallet, C. Woywod, H. Köppel, and W. Domcke, "Multimode Jahn–Teller and pseudo-Jahn–Teller coupling effects in the photoelectron spectrum of CH_3F," *Chemical Physics*, vol. 304, pp. 17–34, sep 2004.

[57] E. Hirota, K. Kawaguchi, T. Ishiwata, and I. Tanaka, "Vibronic interactions in the NO_3 radical," *The Journal of Chemical Physics*, vol. 95, pp. 771–775, jul 1991.

[58] U. Höper, P. Botschwina, and H. Köppel, “Theoretical study of the Jahn–Teller effect in $\tilde{X}^2E$ CH_3O,” *The Journal of Chemical Physics*, vol. 112, pp. 4132–4142, mar 2000.

[59] E. Haller, H. Köppel, L. S. Cederbaum, W. von Niessen, and G. Bieri, “Multimode Jahn–Teller and pseudo-Jahn–Teller effects in BF_3^+,” *The Journal of Chemical Physics*, vol. 78, pp. 1359–1370, feb 1983.

[60] C. Woywod, S. Scharfe, R. Krawczyk, W. Domcke, and H. Köppel, “Theoretical investigation of Jahn–Teller and pseudo-Jahn–Teller interactions in the ammonia cation,” *The Journal of Chemical Physics*, vol. 118, pp. 5880–5893, apr 2003.

[61] A. Viel, W. Eisfeld, S. Neumann, W. Domcke, and U. Manthe, “Photoionization-induced dynamics of ammonia: Ab initio potential energy surfaces and time-dependent wave packet calculations for the ammonia cation,” *The Journal of Chemical Physics*, vol. 124, p. 214306, jun 2006.

[62] T. S. Venkatesan and S. Mahapatra, “Exploring the Jahn-Teller and pseudo-Jahn-Teller conical intersections in the ethane radical cation,” *The Journal of Chemical Physics*, vol. 123, p. 114308, sep 2005.

[63] A. Meurer, C. P. Smith, M. Paprocki, O. Čertík, S. B. Kirpichev, M. Rocklin, A. Kumar, S. Ivanov, J. K. Moore, S. Singh, T. Rathnayake, S. Vig, B. E. Granger, R. P. Muller, F. Bonazzi, H. Gupta, S. Vats, F. Johansson, F. Pedregosa, M. J. Curry, A. R. Terrel, Š. Roučka, A. Saboo, I. Fernando, S. Kulal, R. Cimrman, and A. Scopatz, “SymPy: symbolic computing in Python,” *PeerJ Computer Science*, vol. 3, p. e103, jan 2017.

[64] T. E. Oliphant, *Guide to NumPy*. USA: CreateSpace Independent Publishing Platform, 2nd ed., 2015.

[65] H. Weyl, *The Classical Groups: Their Invariants and Representations*. Princeton University Press, 1946.

[66] D. Opalka and W. Domcke, “High-order expansion of $T_2 \otimes t_2$ Jahn–Teller potential-energy surfaces in tetrahedral molecules,” *The Journal of Chemical Physics*, vol. 132, p. 154108, apr 2010.

[67] D. Opalka and W. Domcke, “High-order expansion of $T_2 \otimes e$ Jahn–Teller potential-energy surfaces in tetrahedral systems,” *Chemical Physics Letters*, vol. 494, no. 4, pp. 134 – 138, 2010.